ACS APPLIED MATERIALS & INTERFACES

Research Article

www.acsami.org

Exploring and Exploiting the Effect of Solvent Treatment in Membrane Separations

Mayamin Razali,[†] Christos Didaskalou,[†] Jeong F. Kim,[‡] Masoud Babaei,[†] Enrico Drioli,[‡,§] Young Moo Lee,[‡] and Gyorgy Szekely*[,†]

[†]School of Chemical Engineering & Analytical Science, The University of Manchester, The Mill, Sackville Street, Manchester M13 9PL, United Kingdom

[‡]WCU Department of Energy Engineering, Hanyang University, 222 Wangsimni ro, Seongdong-gu, Seoul 04763, Republic of Korea

[§]Institute on Membrane Technology (ITM-CNR), Via P. Bucci 17/C, 1-87030 Rende, Cosenza, Italy

Supporting Information

ABSTRACT: It is well-known that solvent treatment and preconditioning play an important role in rejection and flux performance of membranes due to solvent-induced swelling and solvent adsorption. Investigations into the effect of solvent treatment are scarce and application specific, and were limited to a few solvents only. This study reveals the trend in solvent treatment based on solvent polarity in a systematic investigation with the aim to harness such effect for intensification of membrane processes. Nine solvents with polarity indices ranging from 0.1 to 5.8 (hexane to acetonitrile) were used as treatment and process solvents on commercial Borsig GMT-oNF-2, Evonik Duramem 300, and emerging tailor-made polybenzimidazole membranes. TGA-GCMS, HS-GC-FID, and NMR techniques were employed to better understand the effect of solvent treatment on the polymer matrix of membranes. In this work, apart from the solvent treatment's direct effect on the membrane performance, a subsequent indirect effect on the ultimate separation process was observed. Consequently, a pharmaceutical case study employing chlorhexidine disinfectant and antiseptic was used to demonstrate the effect of solvent treatment on the nanofiltration-based purification. It is shown that treatment of polybenzimidazole membranes with acetone resulted in a 25% increase in product recovery at 99% impurity removal. The cost of the process intensification is negligible in terms of solvent consumption, mass intensity, and processing time.

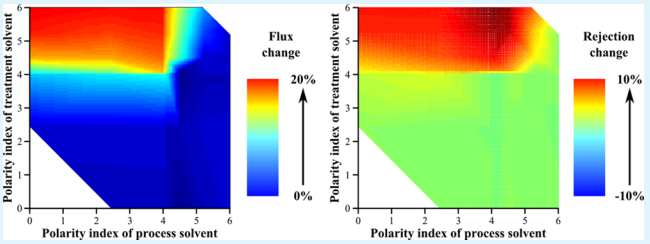

KEYWORDS: *membrane conditioning, process intensification, nanofiltration, pharmaceuticals, membrane preconditioning*

1. INTRODUCTION

In the past 2 decades significant works have been carried out to develop solvent resistant membranes and to ultimately design separation processes in organic media.[1] Organic solvent nanofiltration (OSN) is considered as a sustainable alternative to conventional separation techniques with an evolving range of applications around recovery of products, catalysts, and solvents.[2] Recent developments in the field provided membranes with long-sought-after properties of stability in harsh environments including polar aprotic solvents and extreme pH, high flux, and low molecular weight cutoff (MWCO).

Prior to using OSN membranes, it is necessary to first condition the membranes, typically referred to as solvent treatment. The purpose of this treatment is 2-fold. First, it ensures stable separation performance with regard to solvent flux and solute rejection. Second, it washes out any leachable additives such as pore preservatives and surface modification agents and consequently prevents contamination of the system. The membrane conditioning step is particularly important in the field of OSN. It has been well-documented that solvents, depending on their chemical properties, interact differently with membranes.[3,4] Consequently, initial solvent treatment significantly affects the OSN performance; however, out of the four pillars necessary to gain full control over OSN (Figure 1), membrane conditioning is the least studied and it is the focal point of this study.

Since most liquid-based membrane operations focus on water applications, there is yet a lack of detailed understanding on the underlying effects of solvents on membrane performance. It has been reported that the chemistry of the solvent plays a critical role in membrane performance in terms of flux and retention properties. Gibbins et al. first recognized that the inconsistencies in the reported flux data arise due to different membrane conditioning protocols (different solvent treatments).[3] Van der Bruggen et al. revealed that solvent treatment for 24 h immersion in the solvent used for the measurements reduced the ethanol and hexane flux for the hydrophobic

Received: February 8, 2017
Accepted: March 9, 2017
Published: March 9, 2017

DOI: 10.1021/acsami.7b01879
ACS Appl. Mater. Interfaces 2017, 9, 11279−11289

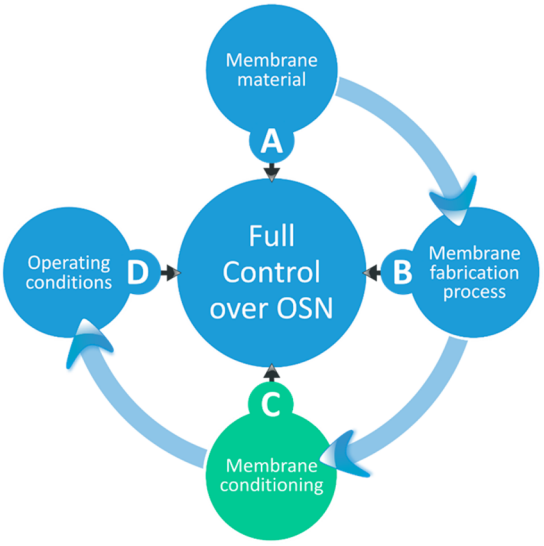

Figure 1. Full control over organic solvent nanofiltration can be achieved through the understanding of (A) the membrane material, (B) the membrane fabrication process, (C) membrane conditioning or solvent treatment, and (D) the operating conditions. Membrane conditioning, aka solvent treatment, is the least studied of the four pillars allowing full control over OSN operations.

membrane (Koch MPF-50), but increased the solvent flux for the hydrophilic membranes (Koch N30F, NF-PES-10, and MPF-44).[4] Such observation was dedicated to the changes in the membrane structure by the solvent treatment having a significant effect on the membrane performance.

More recently, a breakthrough observation was reported by Jimenez-Solomon et al.,[5] that thin film composite (TFC) membranes can be "solvent activated" with DMF. For instance, the acetone flux through the prepared TFC (polyamide) remarkably improved from 0.3 to 71.0 $L{\cdot}m^{-2}{\cdot}h^{-1}$ at 30 bar. However, it should be noted that this solvent activation was due to the removal of the unreacted monomers from the membrane top layer blocking the membrane, and this phenomenon does not universally apply to all TFC membranes. Nonetheless, such activation protocol has also shown similar efficacy in reverse osmosis membranes where the water permeance increased from 0.2 to 1.6 $L{\cdot}m^{-2}{\cdot}h^{-1}{\cdot}bar^{-1}$.[6]

The pioneering work by Machado et al. revealed the complex and nonlinear nature of solvent properties and solvent flux through OSN membranes,[7] and subsequent works attempted to describe their correlation using various models.[3,4,8−10] However, membrane conditioning is yet to be investigated systematically as only a few studies focused on solvent treatment and they were limited to ultrafiltration[11−13] and pervaporation.[14] Nevertheless, solvent treatment by immersion into the process solvent was often used to stabilize solvent flux.[15−17] The first detailed investigation about solvent treatment of OSN membranes was carried out by Zhao and Yuan concluding that methanol and acetone treatment results in significant changes of both solvent flux and solute rejection due to the swelling of polyamide- and polyimide-based membranes.[18] The authors speculated that the polymers have strong interactions with these solvents which could cause changes in hydrophobicity, pore size, and free volume.

Darvishmanesh et al. investigated for the first time the treatment effect of solvent other than the process solvent.[19] Treatment with polar solvents (methanol, acetone, and acetic acid) resulted in lower dye rejections and higher solvent fluxes using polyimide-based Starmem membranes in toluene. On the contrary, nonpolar solvents did not change the polyimide membrane performance significantly. Contact angle and swelling measurements confirmed the membrane structure changed after the solvent treatment due to polymeric network chain rearrangement. Interestingly, it has been shown that such swelling of polymeric network can be exploited by applying nanofiltration membranes to pervaporation applications.[20]

Until now, the effect of solvent treatment on OSN membrane performance has mainly been studied on polyimide membranes. In this work, we systematically investigated the solvent effect on three different types of OSN membranes: polybenzimidazole (PBI), polyimide, and polydimethylsiloxane (PDMS) materials (Table 1). Nine different types of organic

Table 1. Summary of Tested Membranes

Membrane	Manufacturer	Active layer	Contact angle (deg)	Structure
DuraMem300	Evonik MET	Polyimide (crosslinked)	59	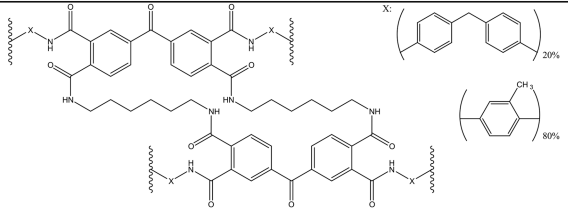
GMT-oNF-2	Borsig GmbH	PDMS	87	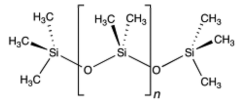
PBI26DBX	In-house fabricated	PBI (crosslinked)	34	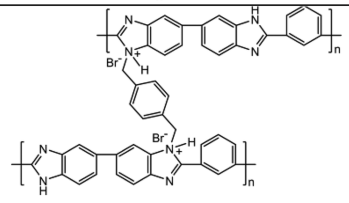

DOI: 10.1021/acsami.7b01879
ACS Appl. Mater. Interfaces 2017, 9, 11279−11289

Table 2. Treatment and Process Solvents and Their Properties (MW = Molecular Weight, THF = Tetrahydrofuran, EtOAc = Ethyl Acetate, DCM = Dichloromethane, and IPA = Isopropyl Alcohol)

Solvent	Abbreviation	Polarity Index	MW ($g \cdot mol^{-1}$)	Specific Density ($g \cdot mL^{-1}$)	Surface Tension ($dyne \cdot cm^{-1}$)	Viscosity (cP)
Acetonitrile	S1	5.8	41.1	0.779	28.7	0.37
Methanol	S2	5.1	32.0	0.787	22.1	0.54
Acetone	S3	5.1	58.1	0.786	23.0	0.31
EtOAc	S4	4.4	88.1	0.894	23.2	0.42
THF	S5	4.0	72.1	0.9	26.7	0.5
IPA	S6	3.9	60.1	0.783	23.3	2.04
DCM	S7	3.1	84.9	1.318	27.8	0.41
Toluene	S8	2.4	92.1	0.865	27.9	0.56
Hexane	S9	0.1	86.2	0.655	18.0	0.3

solvents with varying polarity index have been tested (Table 2). Treatment solvents (TSs) and process solvents (PSs) are defined as solvents used for conditioning the membranes and used as media for the separation process, respectively. In order to elucidate the underlying basis behind the solvent effect, we have applied various analytical techniques to understand the changes at the molecular level.

Solvent treatment has a direct effect on membrane performance and indirectly affects the ultimate process performance. Consequently, in this work, we show that the effect of solvent treatment can be tailored to improve the separation yield of a pharmaceutical purification case study. Genotoxins are often present in crude pharmaceutical streams posing a significant risk to patients.[21] Regulatory authorities and manufacturers are in agreement that the formation or use of these compounds should be avoided in the first place. However, such a preventive approach is not always possible which requires the purging of impurities to a safe level. Hence, OSN was recently proposed as a general platform for the mitigation of genotoxic impurities.[22] A pharmaceutical purification case study was provided by SMR Maju Resources to evaluate the potential of nanofiltration for replacing conventional extraction and recrystallization with the aim to achieve process intensification. The case study of chlorhexidine synthesis[21] depicted in Scheme 1 was selected to demonstrate that the effect of solvent treatment can be exploited for enhancing separation performance.

2. EXPERIMENTAL SECTION

2.1. General Methodology. Chemicals (reagent grade) and solvents (analytical grade) were purchased from Sigma–Aldrich (U.K.) and Fisher Scientific (U.K.), respectively. A 26 wt % amount of PBI (MW = 27,000 $g \cdot mol^{-1}$) containing 1.5 wt % lithium chloride (stabilizer) dissolved in *N*,*N*-dimethylacetamide (DMAc) solution was purchased from PBI Performance Products Inc. (USA). Nonwoven polypropylene fabric Novatexx 2471 was sourced from Freudenberg Filtration Technologies (Germany). GMT-oNF-2 and DuraMem300 can be purchased from Borsig GmbH and Evonik, respectively. Millipore type II water was used for the coagulation bath. Infrared spectra were recorded on a Bruker Alpha-T FT-IR spectrometer. An Agilent 6890N GC system equipped with a Variant Factor 4 VF-5 ms (28 m × 0.25 mm DI × 1 μm DF) column and Agilent 5973 MS detector were used for 2-ethoxyethanol analysis. 4-Chloroaniline and chlorhexidine were analyzed with an Agilent HPLC model 1100 Series system. NMR spectra were recorded in dimethyl sulfoxide-d_6 on a Bruker DRX-500 Avance spectrometer. Membrane samples for NMR were dissolved in dimethyl sulfoxide-d_6 at 80 °C in a sealed container.

2.2. Membrane Fabrication. PBI membranes were fabricated via phase inversion based on the protocol by Valtcheva et al.[23] Dope solutions of 26 wt % were cast onto polypropylene nonwoven sheets using a casting knife set to a thickness of 100 μm at a temperature of 20 °C. Membranes were cast using an automatic film applicator Elcometer 4340. The polymer membranes were then precipitated from solution via immersion into a water bath. The membranes were then placed in isopropyl alcohol (IPA) to remove water from the polymer matrix followed by cross-linking with 3 wt % solutions of α,α'-dibromo-*p*-xylene (DBX) in acetonitrile at 75 °C for 24 h (Scheme 2). The cross-linked membranes were subsequently washed with IPA to remove excess cross-linking agent and then used directly.

2.3. Solvent Treatment Tests. Membranes were conditioned via the continuous permeation of *treatment solvent* at a given pressure (10–30 bar) for 24 h in a cross-flow membrane rig. The process configuration for the membrane conditioning, i.e., solvent treatment, is shown in Figure S1 in the Supporting Information. The system was then drained, refilled with *process solvent*, and conditioned via the continuous permeation of PS at the same pressure for 24 h. Solvent fluxes of each membrane were measured. Then, 10 and 1 $g \cdot L^{-1}$ product (chlorhexidine) and impurities (4-chloroaniline and 2-ethoxyethanol) were loaded into the system and recirculated for 24 h after which solute concentrations were measured and rejections calculated. The full list of experiments is shown in Table S1 in the Supporting Information.

2.4. Purification of Chlorhexidine via Diafiltration. A typical single stage diafiltration system was set up as described elsewhere.[22] The process configuration for the diafiltration is shown in Figure S2 in the Supporting Information. Acetone treatment solvent was recirculated (V_{system} = 0.2 L) for 24 h at 30 bar in a nanofiltration rig containing a 104 cm^2 PBI membrane. Acetone was removed from the system, and one diavolume of IPA was used to remove any remaining treatment solvent. Amounts of 10 and 1 $g \cdot L^{-1}$ product (chlorhexidine) and impurities (4-chloroaniline and 2-ethoxyethanol) were loaded into the rig, and diafiltration was performed in IPA at 30 bar. After 12 diavolumes (2.4 L), the diafiltration was stopped and the rig was drained. Without any treatment, a new batch of crude pharmaceutical was loaded and the diafiltration was repeated. A

Scheme 1. Final Synthetic Step of Disinfectant and Topical Antiseptic Chlorhexidine[a]

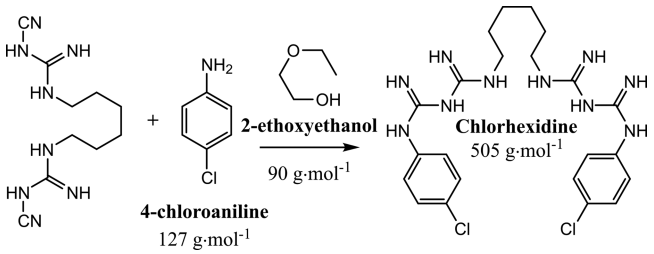

[a]The use of toxic 4-chloroaniline and 2-ethoxyethanol in the final synthetic step of the manufacturing process requires the purging of these impurities.[21]

DOI: 10.1021/acsami.7b01879
ACS Appl. Mater. Interfaces 2017, 9, 11279–11289

Scheme 2. Cross-Linking of Polybenzimidazole with α,α′-Dibromo-*p*-xylene[a]

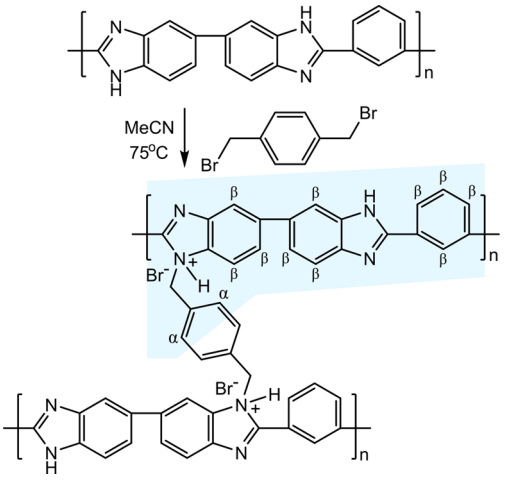

[a]Highlighted substructure represents a monomer unit of the cross-linked PBI. α and β indicate the aromatic protons of the cross-linker and the PBI, respectively.

control experiment was performed following the same procedure with the exception of the treatment solvent (acetone); i.e., no solvent exchange was performed.

2.5. TGA-GCMS Analysis. The membrane sample was removed from the solvent, blotted dry, and placed immediately in the TGA platinum sample pan. For mass and temperature equilibration ca. 2 min elapsed prior to commencement of data recording. TGA measurements were carried out in two successive steps with the same specimen. In the first step, the isothermal weight loss was recorded over 24 h. The sample was kept at a constant 25 °C under helium atmosphere (40 mL·min^{-1}). In the following step, the same specimen was heated to 625 °C at a rate of 20 °C·min^{-1}. The evaporated compounds are transferred by helium carrier gas from the TGA to the GCMS. Mixtures of substances retained from a decomposition step were separated on an Agilent DB-624UI column (30 m × 0.53 mm I.D., 3.0 μm film) and the components were identified in the MS individually. GC oven conditions were as follows: 40 °C//20 min//10°/min//200 °C//20 min; carrier gas, helium 32 cm·s^{-1} (approximately 5 mL·min^{-1}) set at 40 °C.

2.6. HS-GC-FID Analysis. Membrane samples were dried at 25 °C over 24 h. A 100 mg amount of dried membrane samples was placed in 25 mL headspace vials followed by their sonication assisted degradation in 5 mL of DMSO over 60 min. Headspace samples were analyzed by gas chromatography on a Varian CP3800 GC system equipped with an FID detector, a CombiPal autosampler and a DB-ALC1 column (30 m × 0.53 mm; 3.00 μm film thickness; Agilent). In this method the injector temperature was at 35 °C, with a carrier gas of helium (flow rate, 1.5 mL·min^{-1}) and a pressure of 5.1 psi. The program began at 35 °C with a hold for 5 min followed by an increase of temperature to 250 °C at a rate of 40 °C·min^{-1}. The FID detector was maintained at a temperature of 250 °C with a flow of hydrogen at 30 mL·min^{-1}.

3. RESULTS AND DISCUSSION

3.1. Effect of Solvent on Membrane Performance. In order to set a benchmark in membrane performance, the solute rejections for the chlorhexidine, 4-chloroaniline, and 2-ethoxyethanol model system and the solvent permeances were determined and the results are summarized in Figure 2. It can be seen that the membrane performance varies widely among the tested membranes. For instance, Figure 2A shows that the permeance of DM membrane monotonously decreases as the polarity of the solvent decreases (S1 → S9). In the case of PBI membrane, there is also an inverse trend in permeability

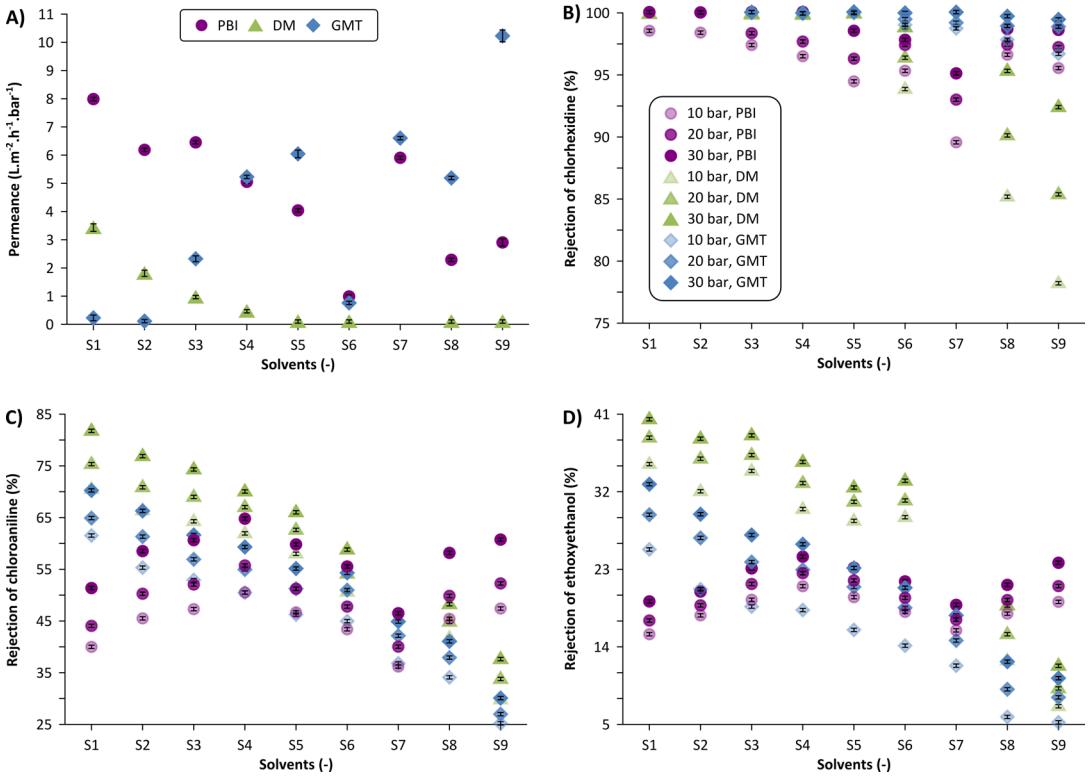

Figure 2. Permeance (A) and rejection (B–D) performance of nontreated polybenzimidazole (PBI), Duramem 300 (DM), and GMT-oNF-2 (GMT) membranes.

DOI: 10.1021/acsami.7b01879
ACS Appl. Mater. Interfaces 2017, 9, 11279–11289

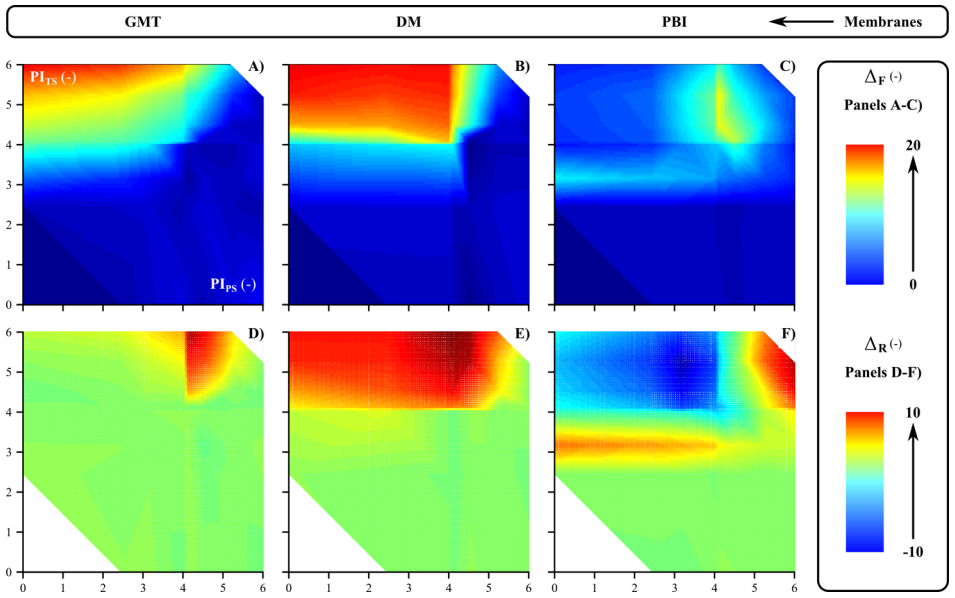

Figure 3. Effect of polarity indices of treatment (PI_{TS}) and process (PI_{PS}) solvents on (A–C) solvent flux (ΔF) and (D–F) solute rejection of 4-chloroaniline (ΔR) at 30 bar for GMT, DM, and PBI membranes.

with increasing solvent polarity. On the contrary, the hydrophobic GMT membrane exhibits an increase in permeability with decreasing solvent polarity, confirming that the polymer–solvent interaction is one of the key parameters in membrane flux.[10] As summarized in Table 1, the contact angle of GMT membrane is higher compared to those of DM and PBI membranes, partly explaining the observed trend that membrane hydrophilicity affects the observed flux. Notably, the flux for IPA was low for all three tested membranes, likely due to the high solvent viscosity of IPA compared to other solvents (see Table 2).

The tested membranes also showed different rejection profiles. In the field of nanofiltration, the transport mechanism lies between the solution-diffusion and pore-flow models.[1] Moreover, in the field of OSN, the membranes, depending on their material properties, show drastically different trends. Although there have been many efforts to understand and predict the OSN rejection profiles,[24−26] the practice now is largely heuristic and is only understood using phenomenological models. For instance, in the case of DM membranes, it can be seen in Figure 2B–D that the solute rejection drops with decreasing solvent polarity and with decreasing solvent flux. The change in rejection is significant for 4-chloroaniline from 80% to 35% as the solvent flux decreased. Such a trend can be qualitatively rationalized using the solution-diffusion model where the decrease in partial flux of the solvent at constant partial solute flux lowers the apparent solute rejection.[27] That is, the relative permeation of solvent decreased as the solvent became less polar, lowering the apparent solute rejection (the definition of rejection is one minus the ratio of permeate and retentate *concentration*). In addition, the work presented by Buekenhoudt et al., reported a similar trend where solute retention decreases with decreasing solvent polarity.[28] The work proposed that Spiegler-Kedem theory on porous membrane morphology well-describes the observed phenomenon, assuming that no swelling takes place.

On the other hand, PBI membranes gave similar rejections regardless of the solvent media, suggesting that the rejection mechanism is largely due to size exclusion (i.e., pore-flow model applies). Interestingly, the GMT membranes showed a combined behavior where the rejection of chlorhexidine (505 g·mol^{-1}) occurred via size exclusion mechanism and the rejections of 4-chloroaniline (127 g·mol^{-1}) and 2-ethoxyethanol (90 g·mol^{-1}) decreased with decreasing solvent polarity (note that the flux *increases* with decreasing solvent polarity). Such a decrease in solute rejections with decreasing solvent polarity may be dedicated to the change in solute–membrane interaction in the presence of nonpolar solvent. However, the rejection profile is difficult to predict, and the explanation relied largely on using phenomenological models.

3.2. Phenomenological Effects of Solvent Treatment on Membrane Performance. The two-phase (liquid, solid) and four-component (treatment solvent, process solvent, solute, and membrane) system is intrinsically complex in nature, making it difficult to draw universal conclusions. The main purpose of this section is to elucidate the effects of solvent treatment on membrane performance. The screening data set presented in Figure 2 was used to compare against the performance of solvent-treated membranes. The change in rejection was calculated as the difference between the rejections with and without solvent treatment and defined in eq 1:

$$\Delta R_x^i/\% = \frac{R_{x,\text{treated}}^i - R_{x,\text{nontreated}}^i}{R_{x,\text{nontreated}}^i} \times 100 \quad (1)$$

where R is the rejection of compound i using membrane x with or without solvent treatment. In order to show the effect of pressure on solvent treatment, the change in flux is calculated as defined in eq 2:

$$\Delta F_x/\% = \frac{F_{x,\text{treated}} - F_{x,\text{nontreated}}}{F_{x,\text{nontreated}}} \times 100 \quad (2)$$

where F is the solvent flux of membrane x with or without solvent treatment. Table S1 lists all the experiments, while the surface plots in Figure S3 summarize the effect of solvent treatment for each membrane in 3 × 4 matrices (see Supporting Information). The performance change of the GMT (Figure S3A) and DM (Figure S3B) membranes shows a

DOI: 10.1021/acsami.7b01879
ACS Appl. Mater. Interfaces 2017, 9, 11279–11289

similar trend. However, the latter is more pronounced. The higher the polarity of the treatment solvent, the larger the effect on flux. It can be also deduced from the 3D plot that the flux for low polarity process solvents show more pronounced effects. The dissimilar behavior observed for the GMT−DM pair and the PBI could be attributed to the fact that the former two are formed by neutral polymers while the cross-linked PBI is ionic featuring a quaternary ammonium salt moiety ($\equiv NH^+Br^-$).[29] The contour plots in Figure 3 show the main solvent treatment effects through representative examples from Figure 3S in the Supporting Information.

Flux. Treatment solvents with high polarity index ($PI_{TS} > 4$) increase the flux of the membranes by up to 17.5% (DM, PI_{TS} = 5.1, PI_{PS} = 0.1, 30 bar). Additionally, the extent of flux increase depends not exclusively on the membrane but on the process solvent as well: the lower the polarity index of the process solvent, the higher the effect. For instance, methanol as treatment solvent (PI_{TS} = 5.1) for the GMT membrane at 30 bar increased the flux for process solvents hexane (PI_{PS} = 0.1) and ethyl acetate (PI_{PS} = 4.4) by 14.2% and 7.3%, respectively. At the same time the solute rejections remained virtually unchanged. The generally sought-after flux enhancement for low polarity solvents can be realized with DM (polyimide) and GMT (PDMS) membranes via high polarity solvent treatment without compromising rejection (Figure 3A,B). For instance, treating the GMT and DM membrane with acetonitrile (PI_{TS} = 5.8) at 30 bar improved the hexane flux by 17%. On the contrary, the prediction of solvent treatment induced flux change for PBI membrane is less straightforward. Figure 3F reveals that high polarity treatment solvents did not improve the flux of low polarity process solvents but instead increased the flux of high polarity solvents up to 13% (PBI, PI_{TS} = 5.1, PI_{PS} = 4.0, 30 bar). DCM as treatment solvent (PI_{TS} = 3.1) for PBI shows an anomalous behavior and increases the flux of about 3−5% irrespectively of the process solvents' polarity index. Again, such unpredictable behavior may be attributed to the fact that cross-linked PBI membrane contains quaternary ammonium salt moieties.

Rejection. The same trend was observed for the rejection change profile of all three compounds. The most significant change in rejection was always observed for the medium sized compound, 4-chloroaniline (Figure 3D−F). Notice that its rejection out of the three tested compounds is the closest to the inflection point of the MWCO curve of the membranes and consequently any change in the system would cause a considerable change in rejection. For GMT and DM membranes there is no significant change in rejection except for the region where both treatment and process solvents have high polarity. In particular, the rejection values decrease up to 10% in this region. The region of decreasing rejection for the medium sized 4-chloroaniline compound on the DM membrane is expanded covering the low polarity region of the process solvent (Figure 3E). The only noticeable increase in rejections is attributed to the PBI membrane (Figure 3F). While low polarity treatment solvents (PI < 3) showed no noticeable effect on the rejection, the high polarity treatment solvents (PI > 3) can either decrease or increase rejection. In particular, acetone as treatment solvent can increase rejection by up to 3.9%, 9.7%, and 7.6% for chlorhexidine, 4-chloroaniline, and 2-ethoxyethanol, respectively. The cases where the increase in rejection resulted in 100% product rejection are summarized in Table 3. Although the relative increase in rejection is small, the 100% rejection achieved

Table 3. Selected Solvent Treatments Where 100% Product Rejection Can Be Realized without Compromising Flux Performance[a]

Treatment Solvent	PI_{TS}	Process Solvent	PI_{PS}	$R_{chlorhexidine}$ (%)	$\Delta R^{PBI}_{chlorhexidine}$ (%)	ΔF_{PBI} (%)
S3	5.1	S6	3.9	100	2.8	8.6
S3	5.1	S8	2.4	100	1.6	3.6
S3	5.1	S9	0.1	100	1.4	2.4
S4	4.4	S6	3.9	100	2.5	8.6
S4	4.4	S8	2.4	100	1.6	3.1
S4	4.4	S9	0.1	100	1.4	2.4
S5	4.0	S8	2.4	100	1.6	3.1

[a] $R_{chlorhexidine}$ represents the absolute rejection value for the product while $\Delta R^{PBI}_{chlorhexidine}$ and ΔF_{PBI} indicate the solvent treatment induced an increase in rejection and flux, respectively.

results in virtually no product loss during a diafiltration process. Notice that the flux was not compromised in any of these cases; moreover, flux increase up to 8.6% was observed. Such favorable changes in performance could be harnessed for process intensification purposes.

Pressure. In general, the higher the pressure is, the more pronounced the impact of the treatment solvent on both flux and rejection; i.e., the flux and rejection changes monotonously increase by increasing pressure (see Figure S3 in the Supporting Information). The highest increase in flux and rejection due to the increase in pressure from 10 to 30 bar were found to be 4.2% (PBI, PI_{TS} = 5.1, PI_{PS} = 4.0) and 3.2% (DM, PI_{TS} = 5.1, PI_{PS} = 4.0), respectively. Although these changes are relatively small they can still have a significant impact on an actual membrane separation. For instance, in the case of S3 treatment solvent and S6 process solvent the chlorhexidine rejections were 97.2%, 99.6%, and 100% at solvent treatment pressures of 10, 20, and 30 bar, respectively (PBI, PI_{TS} = 5.1, PI_{PS} = 3.9). Although the pressure-induced increase in rejection is only a few percent, ultimately achieving 100% rejection would lead to a significant increase in diafiltration yield.

3.3. Exploiting the Effect of Solvent Treatment for Process Intensification. Besides the direct effect on membrane performance (section 3.2), solvent treatment can have an indirect effect on the ultimate membrane process performance. The latter is best expressed in process yield and mass intensity. A minor increase of 1−3% in product rejection resulting in 100% absolute rejection (see Table 3) can significantly affect the diafiltration yield, and ultimately the sustainability of the process.[30] In this work, harnessing the positive effect of solvent treatment was demonstrated through a diafiltration-based API purification case study. A crude mixture of 10 $g{\cdot}L^{-1}$ chlorhexidine product having 1 $g{\cdot}L^{-1}$ 4-chloroaniline and 2-ethoxyethanol impurities was loaded onto treated and nontreated PBI membranes and diafiltration was performed to remove 4-chloroaniline and 2-ethoxyethanol from the solution.[31] Based on previous industrial studies and requirements set by regulatory authorities, the threshold concentration for the impurities was set at 10 ppm.[23] Given the smaller size and subsequently lower rejection of 2-ethoxyethanol relative to 4-chloroaniline, the latter impurity determines the processing time, i.e., number of diavolumes.[32] Although the solvent treatment had an adverse effect on impurity removal rate, it is negligible, and 11 diavolumes were needed to achieve the threshold level both with and without solvent treatment (Figure 4). Notably, it can be seen that the solvent treatment

DOI: 10.1021/acsami.7b01879
ACS Appl. Mater. Interfaces 2017, 9, 11279−11289

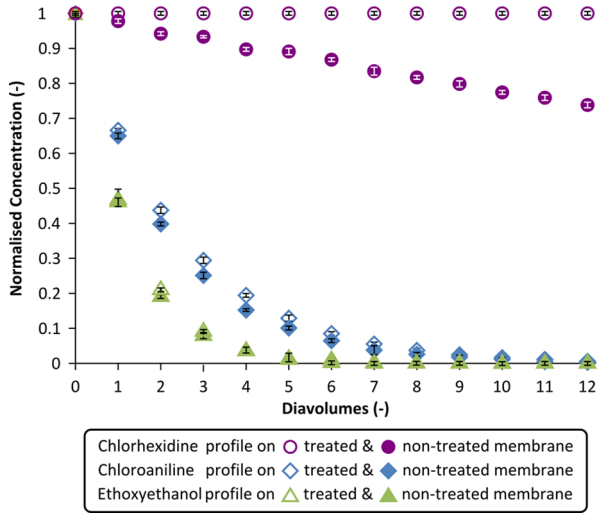

Figure 4. Effect of solvent treatment on the purification of chlorhexidine via diafiltration. While the 4-chloroaniline and 2-ethoxyethanol impurity removal profiles are virtually the same, the product recovery improved about 20%. PBI membrane was employed, operating at 30 bar; acetone and IPA were used as treatment and process solvents, respectively.

increased the product (chlorhexidine) rejection which led to a significant improvement in product yield from 76% to virtually 100%. Moreover, the solvent flux before and after the diafiltration was 20.9 $L{\cdot}m^{-2}{\cdot}h^{-1}$, which is a 9% increase compared to the nontreated membrane. Neither flux decline nor other signs of fouling were observed during the diafiltration.

Figure 5 compares the conventional and nanofiltration assisted downstream processing of chlorhexidine. The currently

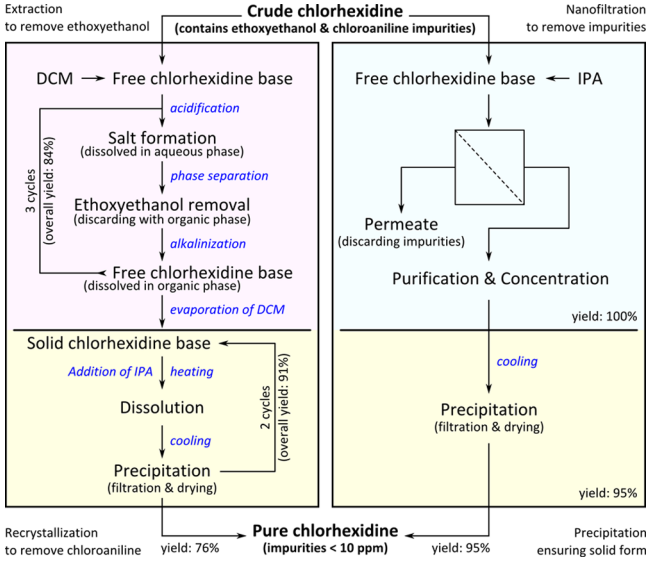

Figure 5. Schematic comparison of conventional purification of chlorhexidine and the OSN-based process.[34]

employed process is comprised of three liquid−liquid extraction cycles and two recrystallization cycles. The optimized process by the manufacturer allows 76% overall yield with less than 10 ppm 2-ethoxyethanol and 4-chloroaniline impurities. On the other hand, the nanofiltration-based process with the incorporation of solvent treatment allows virtually 100% product recovery followed by in situ concentration of the pure product for the final precipitation, yielding 95% product. It should be noted that without the solvent treatment, the yield would only be 76% with membranes (Figure 4). Apart from the yield improvement by solvent treatment, the nanofiltration process has the advantage that both 4-chloroaniline and 2-ethoxyethanol impurities can be removed in a single unit operation *simultaneously*. In addition, the proposed process neither requires any chlorinated solvents nor the acidic and alkaline solutions, reducing the wastewater generation per kg of API from 31 kg to zero. Moreover, the number of unit operations for the downstream processing crude chlorhexidine stream is reduced from 14 to only 2 (diafiltration and precipitation). The process mass intensity (PMI) is the most often used green metric in the pharmaceutical industry to drive more sustainable processes,[33] and it is defined in eq 3:

$$\mathrm{PMI/(kg/kg)} = \frac{\text{total mass in the process}}{\text{mass of product}} \quad (3)$$

The PMI for the conventional process is 662 kg of waste per kg of chlorhexidine. On the other hand, the PMI for the OSN-based process is 238 kg of waste per kg of chlorhexidine, corresponding to a 64% reduction in PMI. Consequently, process intensification via OSN technology for the pharmaceutical industry has been demonstrated.

3.4. Steps toward Better Understanding the Effect of Solvent Treatment. After solvent treatment with acetone and permeation of an excessive amount of IPA, a 10 × 10 mm membrane area was dissolved in DMSO-d_6 in order to investigate the chemical composition of the membrane. The NMR spectra of unused, nontreated but IPA-permeated, and acetone-treated and then IPA-permeated membranes are shown in Figure 6. In the latter case the acetone treatment solvent can

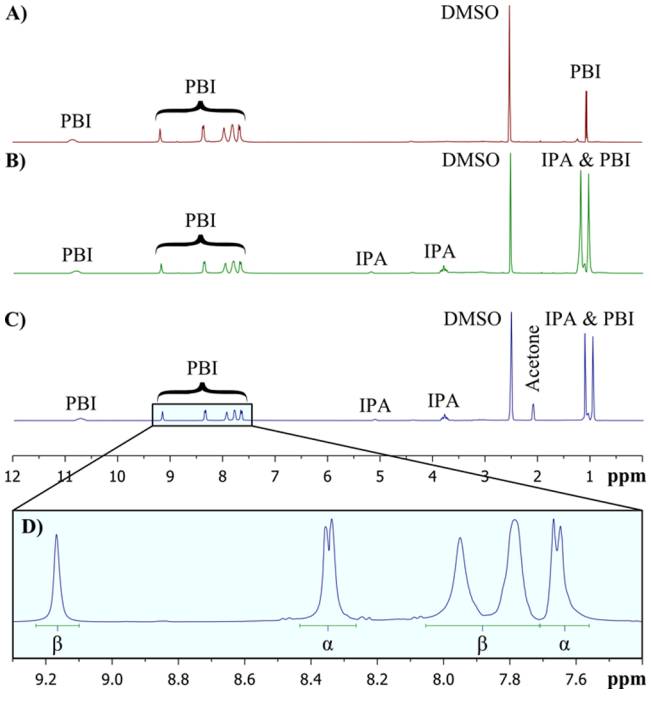

Figure 6. Typical ^{1}H NMR spectra of PBI membranes dissolved in DMSO-d_6 solvent: (A) unused membrane, (B) membrane used for only IPA permeation, (C) membrane treated with acetone followed by diafiltration of IPA, and (D) aromatic region for the cross-linked PBI.

DOI: 10.1021/acsami.7b01879
ACS Appl. Mater. Interfaces 2017, 9, 11279−11289

be found in the membrane material (Figure 6C). Consequently, the acetone treatment solvent was incorporated into the membrane and was not completely washed away even with an excessive amount of IPA (500, 750, and 1000 L·m^{-2}). The chemical shifts of the cross-linker's aromatic protons (indicated as α in Figure 6D) are distinguishable from the aromatic PBI monomer protons (indicated as β in Figure 6D) based on the typical AA′BB′ centrosymmetric spin pattern. α and β protons are indicated in Scheme 2. Calculation of coupling constants is useful in assigning aromatic regions, particularly when chemical shifts between aromatic protons are uncertain or overlapping. In the region of 8.5−7.5 ppm the spectrum contains two doublets with J = 8.1 Hz which falls within the characteristic coupling constant region for hydrogen atoms at the ortho position (6−9 Hz). Consequently, these protons are on a para disubstituted aromatic ring resulting in the AA′BB′ type spin pattern. Only the cross-linker contains protons with such chemical environment (Scheme 2), and thus the integral of the corresponding peaks gives information about the ratio of the cross-linker in the polymer as defined in eq 4:

$$\text{degree of cross-linking} = \frac{A_\alpha {n_\alpha}^{-1}}{A_\beta {n_\beta}^{-1}} \tag{4}$$

where A_α and A_β are the NMR integration areas for the α and β protons, while n_α and n_β are the number of protons. Normalization of the β proton integrals to 10 sets the integral of α and acetone protons to 4.64 ± 0.2 and 2.05 ± 0.1, respectively. The relation between the integrals of β and α patterns revealed that the cross-linker/monomer molar ratio is 1.16 ± 0.1 using eq 4. Furthermore, the relation between the integrals of the β and acetone patterns reveals the PBI monomer/acetone molar ratio to be 2.94 ± 0.13 as per eq 5:

$$\text{degree of acetone adsorption} = \frac{A_{\text{acetone}} {n_{\text{acetone}}}^{-1}}{A_\beta {n_\beta}^{-1}} \tag{5}$$

where A_{acetone} are the NMR integration areas for acetone protons, while n_{acetone} is the number of protons in an acetone molecule. Hence, it can be deduced that three monomer units in the polymer incorporated one acetone molecule. Determination of the degree of cross-linking and incorporation of acetone by the polymer permitted the calculation for the average molecular weight of the cross-linked polymer's monomer unit to be 449 ± 3 g·mol^{-1} as per eq 6:

$$\text{MW}/(\text{g·mol}^{-1}) = \text{MW}_{\text{PBI}} + \frac{A_\alpha {n_\alpha}^{-1}}{A_\beta {n_\beta}^{-1}} \text{MW}_{p\text{-xylyl}} + \frac{A_{\text{acetone}} {n_{\text{acetone}}}^{-1}}{A_\beta {n_\beta}^{-1}} \text{MW}_{\text{acetone}} \tag{6}$$

where MW_{PBI}, $\text{MW}_{p\text{-xylyl}}$, and $\text{MW}_{\text{acetone}}$ are the molecular weights for the PBI monomer prior to cross-linking, the p-xylyl unit of cross-linked PBI bearing the α protons, and the acetone, respectively.

Valuable information about membrane structure and thermal stability can also be obtained by means of thermogravimetric analysis (TGA). For deeper analysis of the pyrolysis products, a GCMS was linked with TGA, forming a powerful analytical tool (TGA-GCMS) for elucidation of pyrolysis degradation products. The TGA weight loss profiles are shown in Figure 7. An isothermal weight loss profile was observed at room temperature which can be attributed to the loss of the

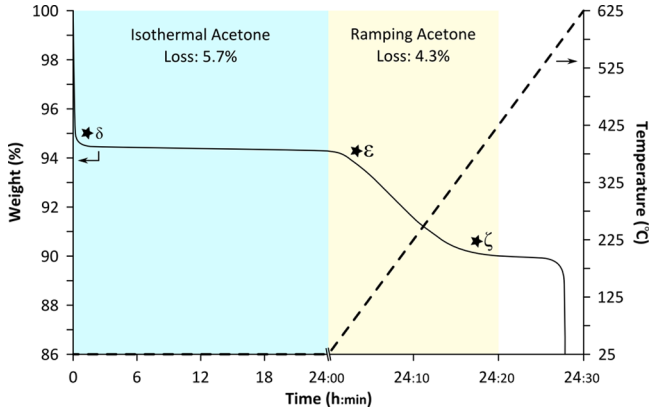

Figure 7. Typical TGA weight loss profile of acetone-treated PBI membrane: isothermal weight loss of acetone for 24 h and consecutive temperature domain weight loss of the membrane. Sample taking points for GCMS analysis are indicated with stars. The volume of IPA used for the washing of the acetone-treated membrane was 500 L·m^{-2}.

nonbound acetone from the surface of the membrane. As described in the Experimental Section, sample handling and instrument equilibration introduce a "dead time" of approximately 2 min. It is reasonable to assume that some of the surface acetone is lost during this dead time and consequently the total amount of surface acetone cannot be measured. However, to determine the total "bonding acetone" (acetone molecules embedded in the structure, bonding with the polar moieties of the polymer), the temperature-dependent TGA measurement is indispensable. The subsequently measured temperature-dependent weight loss profile of the same sample revealed the amount of acetone bound to the membrane. δ, ε, and ζ gas chromatograms and the mass spectra of the corresponding peaks taken at each decomposition step confirmed that the main component was acetone (Figure 8). Particularly, the ramping acetone loss contained 98.5 ± 0.4% acetone and in total 1.6 ± 0.4% DMAc and acetonitrile which were used during the fabrication of the membrane as dope solution solvent and cross-linking solvent, respectively. Based on the total polymer mass and loss of bound acetone, the PBI monomer/acetone molar ratio can be calculated as 3.09 ± 0.25 which is in good agreement with the 2.94 ± 0.13 value derived from the NMR measurements.

Headspace gas chromatography coupled with flame ionization detector (HS-GC-FID) was used as an alternative method to quantify the bound acetone treatment solvent. Unused, nontreated, and acetone-treated membranes were dissolved in DMSO, and the headspace revealed the amount of acetone in the sample (Figure 9). The acetone concentration was found to be 0.78 ± 0.04 g·L^{-1}. The subsequently derived PBI monomer/acetone molar ratio was 3.19 ± 0.16. Further experiments were carried out in which the volume of IPA used for washing of the acetone-treated membrane was 750 and 1000 L·m^{-2}. The acetone content in these membranes were quasi the same (±2%) as with 500 L·m^{-2} washing which indicates that the acetone does not get released from the membrane under the applied conditions. Three independent methods, namely, NMR, TGA, and HS-GC-FID, revealed the molar ratio of the PBI monomer and bound acetone to be 3.07 ± 0.19. The good agreement among the results proves the appropriateness of such methods to be used for the quantification of bound/adsorbed species in the polymer matrix of membranes.

DOI: 10.1021/acsami.7b01879
ACS Appl. Mater. Interfaces 2017, 9, 11279−11289

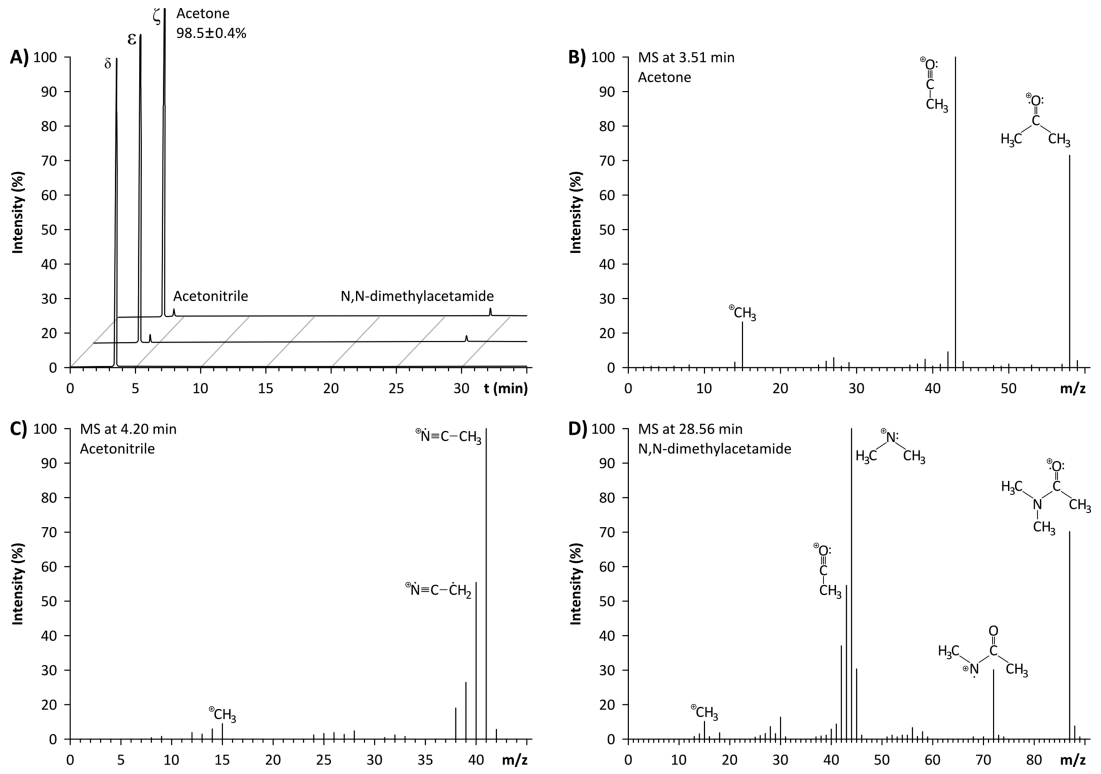

Figure 8. TGA-GCMS results: (A) gas chromatogram and (B–D) corresponding mass spectra of δ, ϵ, and ζ samples taken during different TGA decomposition steps as shown in Figure 7.

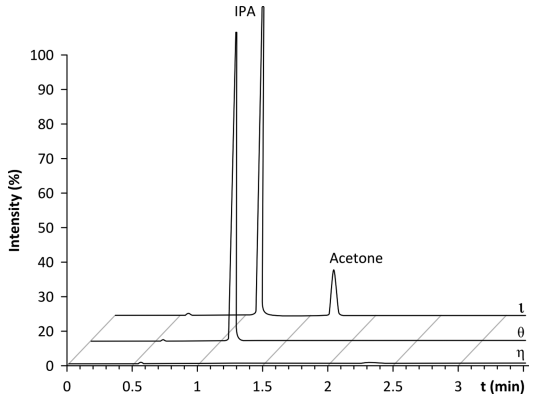

Figure 9. HS-GC-FID chromatograms: η for unused membrane, θ for membrane used for only IPA permeation, ι for membrane treated with acetone followed by diafiltration of 500 L of IPA/(m^2 of membrane).

The change in IPA permeation could be dedicated to the difference in membrane–solvent interaction, which could be semiqualitatively calculated using the solubility parameter approach. The solubility parameter of the PBI and PBI:acetone (3:1) was calculated as shown in Table 4. The solubility parameter was estimated using the group contribution method. The polymer–solvent interaction parameter, χ, is a sum of the enthalpic and entropic components of the polymer–solvent interaction. The lower the value of χ is, the better the interaction between the polymer and the solvent. It can be seen in Table 4 that after the acetone treatment (incorporation of acetone molecule to PBI membrane in 3:1 ratio), the value of χ dropped by 40% (1.27 to 0.75). Although the solubility parameter approach is largely qualitative, the calculation suggests that the affinity of PBI membranes toward IPA significantly increased after the acetone treatment, and consequently explains the observed improvement in solvent permeability. Contact angle measurements revealed a small increase in the hydrophilicity of the membrane surface; however, it is negligible due to the appreciable error in the measurement (Table 4). Elemental microanalysis indicated that the bromine content derived from the cross-linking ($\equiv NH^+Br^-$) of the membrane is quasi constant and not being washed away by the solvents employed, indicating that the bound acetone enhanced the solvent permeability.

Table 4. Estimated Solubility Parameter of PBI, the Interaction Parameter with IPA, Contact Angles, and Bromine Content with (Line No. 1) and without (Line No. 2) Acetone Treatment[a]

no.	$\delta_{dispersion}$ ($MPa^{0.5}$)	δ_{polar} ($MPa^{0.5}$)	$\delta_{hydrogen}$ ($MPa^{0.5}$)	$\delta_{overall}$ ($MPa^{0.5}$)	$\chi_{(PBI-IPA)}$	Contact Angle (deg)	Bromine Content (%)
1	25.50	9.74	9.76	28.99	1.27	34.2 ± 4.3	19.26/19.3 ± 0.2[b]
2	24.05	8.55	9.27	27.16	0.75	30.6 ± 3.2	20.09/19.9 ± 0.2[b]

[a]The contact angles and the bromine content are for individual membranes treated with 500, 750, and 1000 $L \cdot m^{-2}$ IPA, and the found averages with standard deviations are shown in the table. [b]Calculated bromine content based on the results of eqs 4 and 5/measured values from elemental microanalysis.

DOI: 10.1021/acsami.7b01879
ACS Appl. Mater. Interfaces 2017, 9, 11279–11289

4. CONCLUSIONS

In this work, the effect of solvent treatment for OSN performance was systematically studied using three different types of membranes: cross-linked polyimide membrane, cross-linked polybenzimidazole membrane, and polydimethylsiloxane membrane. It has been shown that the OSN membrane performance is considerably affected by the polarity of the treatment solvent and such phenomenon in OSN technology should not be underestimated. Particularly, treating polyimide and PDMS membranes with polar solvents significantly improved the flux of nonpolar solvents without compromising the solute rejections. On the other hand, PBI membrane did not follow the same trend, likely due to its different chemical nature featuring quaternary ammonium salt moieties. In light of our results the design of OSN-based solvent exchange[35,36] and separation of binary solvent mixtures[37,38] should take into account the possible changes in membrane performance. Moreover, during membrane screening and membrane development work, the solvents should not be improvidently exchanged assuming solvent-independent membrane performance. We have shown that such solvent-induced performance change could be exploited to our advantage and achieve notable process intensification of conventional pharmaceutical processes. TGA-GCMS and HS-GC-FID techniques were used for the first time to measure the amount of treatment solvent bound to the polymer matrix of membranes. In addition, NMR was found to be a suitable tool for measuring the degree of cross-linking and the average molecular weight of polymer membranes. Such techniques could be used in general to evaluate additives or cross-linking of polymer membranes.

■ ASSOCIATED CONTENT

Supporting Information

The Supporting Information is available free of charge on the ACS Publications website at DOI: 10.1021/acsami.7b01879.

Solvent treatment experiment list, process configurations for solvent treatment and diafiltration, matrix for polarity indices versus flux and rejection change, and elemental microanalysis (PDF)

■ AUTHOR INFORMATION

Corresponding Author

*E-mail: gyorgy.szekely@manchester.ac.uk. Tel.: +44 (0)161 306 4366.

ORCID

Mayamin Razali: 0000-0003-0517-6120
Young Moo Lee: 0000-0002-5047-3143
Gyorgy Szekely: 0000-0001-9658-2452

Notes

The authors declare no competing financial interest.

■ ACKNOWLEDGMENTS

We are grateful for Jozsef Kupai from the Technical University of Budapest for his assistance with the NMR and TGA-GCMS analysis. Further thanks go to Raphael de Souza Rodrigues from the Federal University of Rio de Janeiro for his help with the solvent treatment study. Useful discussions and analytical insights provided by Peter Pogany from Gedeon Richter Plc are greatly acknowledged. We are thankful for the information and in-kind support provided by SMR Maju Resources for the pharmaceutical case study. This work was supported by the Engineering and Physical Sciences Research Council [BioProNET BIV Nov15 Szekely]; the Biotechnology and Biological Sciences Research Council [BioProNET BIV Nov15 Szekely]; and the Nano-Material Technology Development Program − National Research Foundation of Korea (NRF), the Ministry of Education, Science and Technology [Grant 2012M3A7B4049745].

■ NOMENCLATURE

API = active pharmaceutical ingredient
DCM = dichloromethane
DM = Duramem
DMAc = *N*,*N*-dimethylacetamide
DMSO = dimethyl sulfoxide
GMT = GMT-oNF-2
HS-GC-FID = headspace gas chromatography coupled with flame ionization detector
IPA = isopropyl alcohol
MWCO = molecular weight cutoff
NMR = nuclear magnetic resonance
OSN = organic solvent nanofiltration
PBI = polybenzimidazole
PI_{PS} = polarity index of process solvent
PI_{TS} = polarity index of treatment solvent
TGA-GCMS = thermogravimetric analysis coupled with gas chromatography mass spectrometry
THF = tetrahydrofuran
δ_d = dispersion solubility parameter
δ_p = polar solubility parameter
δ_h = hydrogen bonding solubility parameter
$\delta_{overall}$ = combined solubility parameter
ΔR_x^i = rejection change of compound i using membrane x
ΔF_x = flux change of membrane x
$\chi_{(PBI\text{-}IPA)}$ = polymer−solvent interaction parameter

■ REFERENCES

(1) Marchetti, P.; Jimenez Solomon, M. F.; Szekely, G.; Livingston, A. G. Molecular Separation with Organic Solvent Nanofiltration: A Critical Review. *Chem. Rev.* **2014**, *114*, 10735−10806.

(2) Szekely, G.; Jimenez-Solomon, M. F.; Marchetti, P.; Kim, J. F.; Livingston, A. G. Sustainability Assessment of Organic Solvent Nanofiltration: from Fabrication to Application. *Green Chem.* **2014**, *16*, 4440−4473.

(3) Gibbins, E.; D'Antonio, M.; Nair, D.; White, L. S.; Freitas dos Santos, L. M.; Vankelecom, I. F. J.; Livingston, A. G. Observations on Solvent Flux and Solute Rejection Across Solvent Resistant Nanofiltration Membranes. *Desalination* **2002**, *147*, 307−313.

(4) Van der Bruggen, B.; Geens, J.; Vandecasteele, C. Fluxes and Rejections for Nanofiltration with Solvent Stable Polymeric Membranes in Water, Ethanol and n-Hexane. *Chem. Eng. Sci.* **2002**, *57*, 2511−2518.

(5) Jimenez Solomon, M. F.; Bhole, Y.; Livingston, A. G. High Flux Membranes for Organic Solvent Nanofiltration (OSN)-Interfacial Polymerization with Solvent Activation. *J. Membr. Sci.* **2012**, *423*−*424*, 371−382.

(6) Gorgojo, P.; Jimenez-Solomon, M. F.; Livingston, A. G. Polyamide Thin Film Composite Membranes on Cross-linked Polyimide Supports: Improvement of RO Performance via Activating Solvent. *Desalination* **2014**, *344*, 181−188.

(7) Machado, D. R.; Hasson, D.; Semiat, R. Effect of Solvent Properties on Permeate Flow Through Nanofiltration Membranes. Part I: Investigation of Parameters Affecting Solvent Flux. *J. Membr. Sci.* **1999**, *163*, 93−102.

(8) Machado, D. R.; Hasson, D.; Semiat, R. Effect of Solvent Properties on Permeate Flow Through Nanofiltration Membranes: Part II. Transport Model. *J. Membr. Sci.* **2000**, *166*, 63−69.
(9) Bhanushali, D.; Kloos, S.; Kurth, C.; Bhattacharyya, D. Performance of Solvent-resistant Membranes for Non-aqueous Systems: Solvent Permeation Results and Modelling. *J. Membr. Sci.* **2001**, *189*, 1−21.
(10) Robinson, J. P.; Tarleton, E. S.; Millington, C. R.; Nijmeijer, A. Solvent Flux Through Dense Polymeric Nanofiltration Membranes. *J. Membr. Sci.* **2004**, *230*, 29−37.
(11) Shukla, R.; Cheryan, M. Performance of Ultrafiltration Membranes in Ethanol−Water Solutions: Effect of Membrane Conditioning. *J. Membr. Sci.* **2002**, *198*, 75−85.
(12) Giorno, L.; Mazzei, R.; Oriolo, M.; De Luca, G.; Davoli, M.; Drioli, E. Effects of Organic Solvents on Ultrafiltration Polyamide Membranes for the Preparation of Oil-in-water Emulsions. *J. Colloid Interface Sci.* **2005**, *287*, 612−623.
(13) Penha, F. M.; Rezzadori, K.; Proner, M. C.; Zanatta, V.; Zin, G.; Tondo, D. W.; Vladimir de Oliveira, J.; Petrus, J. C. C.; Di Luccio, M. Influence of Different Solvent and Time of Pre-treatment on Commercial Polymeric Ultrafiltration Membranes Applied to Non-aqueous Solvent Permeation. *Eur. Polym. J.* **2015**, *66*, 492−501.
(14) Nguyen, Q. T.; Favre, E.; Ping, Z. H.; Néel, J. Clustering of Solvents in Membranes and its Influence on Membrane Transport Properties. *J. Membr. Sci.* **1996**, *113*, 137−150.
(15) Dijkstra, M. F. J.; Bach, S.; Ebert, K. A Transport Model for Organophilic Nanofiltration. *J. Membr. Sci.* **2006**, *286* (1−2), 60−68.
(16) Silva, P.; Livingston, A. G. Effect of Solute Concentration and Mass Transfer Limitations on Transport in Organic Solvent Nanofiltration — Partially Rejected Solute. *J. Membr. Sci.* **2006**, *280* (1−2), 889−898.
(17) Ebert, K.; Koll, J.; Dijkstra, M. F. J.; Eggers, M. Fundamental Studies on the Performance of a Hydrophobic Solvent Stable Membrane in Non-aqueous Solutions. *J. Membr. Sci.* **2006**, *285* (1−2), 75−80.
(18) Zhao, Y.; Yuan, Q. Effect of Membrane Pretreatment on Performance of Solvent Resistant Nanofiltration Membranes in Methanol Solutions. *J. Membr. Sci.* **2006**, *280*, 195−201.
(19) Darvishmanesh, S.; Degrève, J.; Van der Bruggen, B. Performance of Solvent-Pretreated Polyimide Nanofiltration Membranes for Separation of Dissolved Dyes from Toluene. *Ind. Eng. Chem. Res.* **2010**, *49*, 9330−9338.
(20) Verhoef, A.; Figoli, A.; Leen, B.; Bettens, B.; Drioli, E.; Van der Bruggen, B. Performance of a Nanofiltration Membrane for Removal of Ethanol from Aqueous Solutions by Pervaporation. *Sep. Purif. Technol.* **2008**, *60*, 54−63.
(21) Szekely, G.; Amores de Sousa, M. C.; Gil, M.; Castelo Ferreira, F.; Heggie, W. Genotoxic Impurities in Pharmaceutical Manufacturing: Sources, Regulations, and Mitigation. *Chem. Rev.* **2015**, *115*, 8182−8229.
(22) Szekely, G.; Bandarra, J.; Heggie, W.; Sellergren, B.; Ferreira, F. C. Organic Solvent Nanofiltration: A Platform for Removal of Genotoxins from Active Pharmaceutical Ingredients. *J. Membr. Sci.* **2011**, *381*, 21−33.
(23) Valtcheva, I. B.; Kumbharkar, S. C.; Kim, J. F.; Bhole, Y.; Livingston, A. G. Beyond polyimide: Crosslinked Polybenzimidazole Membranes for Organic Solvent Nanofiltration (OSN) in Harsh Environments. *J. Membr. Sci.* **2014**, *457*, 62−72.
(24) Yang, X. J.; Livingston, A. G.; Freitas dos Santos, L. Experimental Observations of Nanofiltration with Organic Solvents. *J. Membr. Sci.* **2001**, *190*, 45−55.
(25) Silva, P.; Han, S.; Livingston, A. G. Solvent Transport in Organic Solvent Nanofiltration Membranes. *J. Membr. Sci.* **2005**, *262*, 49−59.
(26) Zhao, Y.; Yuan, Q. A Comparison of Nanofiltration with Aqueous and Organic Solvents. *J. Membr. Sci.* **2006**, *279*, 453−458.
(27) Paul, D. R. Reformulation of the Solution-diffusion Theory of Reverse Osmosis. *J. Membr. Sci.* **2004**, *241*, 371−386.
(28) Hosseinabadi, S. R.; Wyns, K.; Meynen, V.; Buekenhoudt, A.; Van der Bruggen, B. Solvent-Membrane-Solute Interactions in Organic Solvent Nanofiltration (OSN) for Grignard Functionalised Ceramic Membranes: Explanation via Spiegler-Kedem Theory. *J. Membr. Sci.* **2016**, *513*, 177−185.
(29) Valtcheva, I. B.; Marchetti, P.; Livingston, A. G. Crosslinked Polybenzimidazole Membranes for Organic Solvent Nanofiltration (OSN): Analysis of Crosslinking Reaction Mechanism and Effects of Reaction Parameters. *J. Membr. Sci.* **2015**, *493*, 568−579.
(30) Kim, J. F.; Szekely, G.; Valtcheva, I. B.; Livingston, A. G. Increasing the Sustainability of Membrane Processes Through Cascade Approach and Solvent Recovery—Pharmaceutical Purification Case Study. *Green Chem.* **2014**, *16*, 133−145.
(31) Notice that the GMT membrane is also a valid candidate for process development based on Figure 2A. However, the PBI membrane has 26% higher flux at 30 bar than the GMT membrane.
(32) For a 1 L system, 1 L permeation refers to 1 diavolume.
(33) Jimenez-Gonzalez, C.; Ponder, C. S.; Broxterman, Q. B.; Manley, J. B. Using the Right Green Yardstick: Why Process Mass Intensity Is Used in the Pharmaceutical Industry To Drive More Sustainable Processes. *Org. Process Res. Dev.* **2011**, *15*, 912−917.
(34) Information for the conventional process (left panel) is provided by manufacturer SMR Maju Resources, Malaysia.
(35) Sheth, J. P.; Qin, Y.; Sirkar, K. K.; Baltzis, B. C. Nanofiltration-based Diafiltration Process for Solvent Exchange in Pharmaceutical Manufacturing. *J. Membr. Sci.* **2003**, *211*, 251−261.
(36) Lin, J. C. T.; Livingston, A. G. Nanofiltration Membrane Cascade for continuous Solvent Exchange. *Chem. Eng. Sci.* **2007**, *62*, 2728−2736.
(37) Darvishmanesh, S.; Degrève, J.; Van der Bruggen, B. Comparison of Pressure Driven Transport of Ethanol/n-Hexane Mixtures Through Dense and Microporous Membranes. *Chem. Eng. Sci.* **2009**, *64*, 3914−3927.
(38) Li, J.; Wang, M.; Huang, Y.; Luo, B.; Zhang, Y.; Yuan, Q. Separation of Binary Solvent Mixtures with Solvent Resistant Nanofiltration Membranes Part A: Investigation of Separation Performance. *RSC Adv.* **2014**, *4*, 40740−40747.

DOI: 10.1021/acsami.7b01879
ACS Appl. Mater. Interfaces 2017, 9, 11279−11289